

## **GAS-LIQUID MASS TRANSFER: INFLUENCE OF SPARGER LOCATION**

R. Sardeing, J. Aubin, M. Poux and C. Xuereb

Laboratoire de Génie Chimique UMR CNRS 5503, Toulouse, France.

Sardeing R., Aubin J., Poux M. and Xuereb C., 'Gas-Liquid Mass Transfer: Influence of Sparger Location' *Trans IChemE*, 82, A9, 1161-1168, (2004).

## ABSTRACT

The performance of three sparger diameters ( $D_S = 0.6D$ ,  $D_S = D$ ,  $D_S = 1.6D$ ) in combination with three positions (below, above or level with the impeller) for gas-liquid dispersion and mass transfer were evaluated in the case of the Rushton turbine and the A315 propeller in up- or down-pumping mode. The results show that the best results in terms of gas handling and mass transfer capacities are obtained for all impellers with the sparger placed below it and with a diameter at least equal to the impeller diameter. For the sparger position below the agitator, the  $k_La$  values of the Rushton turbine are greater than those of the A315 propeller, whatever the pumping mode. The A315 propeller in up-pumping mode is, however, more economically efficient in terms of mass transfer. In all cases, the up-pumping mode gives better results than the down-pumping one.

## KEYWORDS

mixing; stirred tank; gas-liquid; mass transfer; sparger location; up-pumping; axial flow impeller

## CORRESPONDING AUTHOR'S ADDRESS

Correspondence concerning this paper should be addressed to Dr. C. Xuereb, Laboratoire de Génie Chimique UMR CNRS 5503, 5 rue Paulin Talabot, BP-1301, 31106 Toulouse Cedex 1, France.

E-mail: Catherine.Xuereb@ensiacet.fr

## INTRODUCTION

Fermentation, wastewater aeration, oxidation and hydrogenation represent only a large number of the complex mixing processes where gas dispersion is employed in mechanically agitated tanks. Traditionally, gas dispersion in agitated vessels is carried out using radial disc turbines, such as the Rushton turbine, in conjunction with a ring sparger of diameter smaller than the impeller positioned below the stirrer. However, the mass transfer capacity depends not only on the impeller type (radial, axial or mixed) but also on the sparger design and location.

Nienow *et al.* (1986) found that using large diameter ring spargers ( $1.2D$ ), positioned  $D_T/25$  below the Rushton turbine blades, resulted in an increased gas handling capacity, a higher relative power draw and, as a consequence of these effects, a higher specific mass transfer coefficient. Breucker *et al.* (1988) studied the influence of various sparger designs on the two-phase and three-phase operational behaviour of a number of agitators, including the Rushton turbine, a down-pumping propeller and a down-pumping pitched blade turbine.

They found that 'near-wall' ring spargers were unable to flood the stirrer. This arrangement also resulted in substantially improved suspension behavior. The gas hold-up, however, is lower in this case than with a 'far-wall' ring sparger. Rewatkar and Joshi (1991a, 1993) have tested several sparger types and configurations using a pitched blade turbine in the down-pumping mode. They found that the critical impeller speed for gas dispersion,  $N_{CD}$ , depended on the impeller design, the sparger design, the sparger location and the superficial gas velocity. Among the sparger designs they studied, the concentric ring sparger and the large ring sparger ( $2D$ ) were found to be more energy efficient for an early dispersion of gas. They recommended the use of a large ring sparger ( $2D$ ). Rewatkar and Joshi (1991a, 1993) also found that the value of  $N_{CD}$  increased with decreasing distance between the sparger and the impeller, and this reached a maximum when the gas is sparged above the pitched blade down-pumping turbine. They have shown that the effect of the diameter of the ring sparger was predominant when it exceeds the impeller diameter and placed below and away from the impeller. The values of  $N_{CD}$  were found to be the lowest when the ring diameter is twice the impeller diameter. Rewatkar and Joshi (1991a, 1993) also found that the hole size and the number of holes on the ring sparger have a negligible effect when the sparger is located near the impeller. However, these variables become important when the sparger is located away from the impeller. For such a sparger, the value of  $N_{CD}$  decreases with decreasing orifice size or increasing number of holes. Rewatkar and Joshi (1991b) made the same remarks and conclusions as Rewatkar and Joshi (1991a, 1993) did on the critical impeller speed for gas dispersion. Rewatkar *et al.* (1993) have studied the gas hold-up in gas-liquid reactors using a down-pumping pitched blade turbine with several types and configurations of spargers. Of all the spargers tested, the ring sparger gives the highest gas hold-up: 18 to 25% higher than that obtained when using a single point sparger. They found that a sparger located above the impeller always gives a lower gas hold-up than a sparger located below the impeller. When the sparger diameter is  $0.5D$ , a sparger located closer to the impeller gives a lower gas hold-up than the same sparger located far away from the impeller. For a sparger diameter of  $0.8D$ , the opposite is found. Rewatkar *et al.* (1993) observed that a ring sparger of diameter equal to  $0.8D$  and  $2D$  gives the maximum gas hold-up. The latter is recommended in view of stability. In the case of the ring sparger, a smaller number of holes and holes of a smaller size give a larger gas hold-up. Rewatkar *et al.* (1991) carried out a similar study, whereby a solid suspension was added. They found that the values of the critical impeller speed for solid suspension in the gas-liquid-solid system with a ring diameter of  $2D$  were lower at high superficial gas velocities ( $\geq 0.0094 \text{ m}\cdot\text{s}^{-1}$ ). Bakker and Van den Akker (1994) have used four sparger types and two impellers: a PBT and a propeller in the down-pumping mode. By analysis of the  $P_G/P$  curve, they found that the use of a ring sparger located away from the impeller decreased the amount

of power needed to disperse a certain amount of gas. The authors, however, found no clear effect of the sparger type on the gas hold-up. On the other hand, it was found that the sparger with a diameter of  $0.45D$  gives the best result in terms of mass transfer performance. Mc Farlane *et al.* (1995) have tested several sparger types and configurations using two propellers in the down-pumping mode. They recommend the use of a large ring sparger ( $0.8D$ ) with a large sparger-impeller separation ( $0.6$  to  $0.8C$ ), since the relative power drawn, the gas handling capability and the energy efficiency in dispersing gas are all enhanced. Birch and Ahmed (1996, 1997) have worked with a Rushton turbine and a pitched blade disk turbine in the up-pumping and the down-pumping modes. They tested three sparger diameters and three positions for the sparger: above, level and below the impeller. It was found that the most suitable location for introducing the gas appears to be in the discharge flow of the impeller. The most suitable diameter for the sparger is the larger one:  $1.4D$ . In summary, it may be concluded that 'larger than impeller' sparger is better in terms of gas handling capacities and gas hold-up. However, little information is available in terms of mass transfer performances.

In the present work, the performance of two impellers (an A315 hydrofoil propeller both in the down- and up-pumping modes and a Rushton turbine) with several ring sparger configurations are quantified in terms of the volumetric mass transfer coefficient, the overall transfer efficiency, the standard oxygen transfer rate, as well as the power dissipation. For the down-pumping configuration, the sparger is placed below the propeller and in the up-pumping configuration it is placed above. In the case of the Rushton turbine, the sparger is placed below or level with the turbine in the discharge flow of the agitator. In this latter case, the gas is injected towards either the top or the bottom of the tank.

## **METHODS AND MATERIALS**

### **Equipment & Experimental Conditions**

The experiments were performed in a dished-bottom cylindrical vessel with  $D_T = 0.19$  m with an aspect ratio of 1, i.e. the liquid height ( $H$ ) in the vessel was equal to the tank diameter ( $D_T$ ). The tank was equipped with four baffles ( $b = D_T/10$ ), which were placed  $90^\circ$  from one another, flush against the vessel wall. The impeller clearance was  $C = D_T/3$ , where  $C$  is defined as the distance from the vessel bottom to the lowest horizontal plane swept by the impeller. The performances of two impellers were studied: a 4-bladed A315 hydrofoil (Lightnin) in both the down- and up-pumping modes and a Rushton turbine. In all cases, the impeller diameter was equal to  $D = D_T/2$  and the agitator shaft ( $s = 0.008$  m) extended to the bottom of the vessel.

The experiments were carried out at room temperature and atmospheric pressure. Plain tap water was used as the working fluid (coalescent system) and air was fed into the tank via a ring sparger. Three sparger diameters were used:  $D_s = 0.6D$  (ring S – Small size),  $D_s = D$  (ring M – Medium size),  $D_s = 1.6D$  (ring L – Large size). The sparger placed below the impeller (position b) has a clearance,  $C_s = 0.6C$ , and the air bubbles upwards. This position ‘b’ was chosen following the recommendations of McFarlane *et al.*, 1995. For the sparger located above the impeller (position a, only for A315 propeller) with  $C_s = 0.6C$ , the gas bubbles downwards towards the impeller. This position of the sparger was chosen arbitrarily as it is not a typical configuration and therefore it may not be the optimal position. However, care was taken to place the sparger at distance relatively close to the impeller to promote gas dispersion. When the sparger is placed level with the centreline of the impeller (position l, only for the turbine) with  $C_s = C$ , the gas is bubble either downwards or upwards. All spargers have 43 x 0.0009m diameter holes and the configurations are summarised in Table 1, Table 2 and Figure 1. The impeller rotational speed,  $N$ , remained constant at  $5 \text{ s}^{-1}$  (corresponding to fully developed turbulent flow), whilst the gas flow rate varied between  $0.3 - 3.5 \times 10^{-4} \text{ m}^3 \text{ s}^{-1}$ , which is equivalent to a gas flow number,  $Fl$ , variation from 0.012 to 0.075. The flow number is defined as:

$$Fl = \frac{Q_G}{ND^3} \quad (1)$$

where  $Q_G$  is the gas flow rate.

In addition to the mass transfer experiments, which are detailed below, the power consumption was measured in order to characterise the agitation systems. The power consumption of the agitator, with and without gas, was determined by measuring the restraining torque of the motor. For these experiments, the rotational speed of the agitator was kept constant whilst the gas flow rate was varied. The power consumption in absence of gas was represented as the dimensionless power number  $P_0$ :

$$P_0 = \frac{P}{\rho N^3 D^5} \quad (2)$$

where  $\rho$  is the liquid density.

## Mass Transfer

The volumetric mass transfer coefficient,  $k_L a$ , was measured using a dynamic measurement method, assuming perfect mixing in the liquid phase and the first order no depletion model for the gas phase. The choice of a first order model for the gas phase is justified by the fact that such simplified models still preserve the relative order of merit of agitators, making them useful comparison purposes (Lopes de Figueiredo and Calderbank, 1979).

Furthermore, for low  $k_L a$  values ( $< 0.06 \text{ s}^{-1}$ ), like those obtained in this study, the difference between first and second order (eg. perfectly mixed or plug flow models) methods is negligible (Bakker, 1992).

Tap water was used as the operating fluid and was firstly deoxygenated by bubbling nitrogen through it until the dissolved oxygen concentration,  $C_t$ , was  $\leq 0.2 \text{ mg.l}^{-1}$  using an impeller rotational speed of  $5 \text{ s}^{-1}$ . The increase in  $C_t$  was then measured over time as air re-oxygenated the tank water. The  $k_L a$  was then calculated from:

$$C_t = C^* + \frac{(C^* - C_0)}{1 - k_L a \cdot \tau} (k_L a \cdot \tau e^{-t/\tau} - e^{-k_L a t}) \quad (3)$$

where  $C^*$  is the oxygen concentration at saturation,  $C_0$  is the oxygen concentration at  $t = 0 \text{ s}$  and  $\tau$  is the response time of the oxygen probe. A temperature correction to the  $k_L a$  was then applied using the relation (Bouaifi and Roustan, 1994):

$$(k_L a)_{20^\circ\text{C}} = 1.024^{(20-T)} (k_L a)_T \quad (4)$$

where  $T$  is the temperature of water during the experiment.

Measurements were made for various gas flow rates, ranging from  $0.45 \times 10^{-4}$  to  $3.2 \times 10^{-4} \text{ m}^3 \text{ s}^{-4}$  (0.5 – 4.0 vvm), whilst the impeller speed remained constant at  $5 \text{ s}^{-1}$ . In all cases, a complete dispersion flow regime was obtained.

Using the  $k_L a$  values, an economic performance criterion was deduced in order to compare the efficiencies of the different agitators: the Overall Transfer Efficiency (*OTE*), which represents the mass of oxygen transferred to the liquid per kWh (Bouaifi and Roustan, 1994):

$$OTE = \frac{(3.6 \times 10^6) \times (k_L a)_{20^\circ\text{C}} C_{20^\circ\text{C}}^* V}{P_g} \quad (5)$$

where  $V$  is the volume of liquid in the vessel and  $P_g$  is the gassed impeller power consumption.

## RESULTS AND DISCUSSION

### Power Consumption

The ungasged power numbers of the different agitators studied are shown in Table 3. The results are generally in good agreement with those published in the literature. The power values measured for the A315D are however somewhat greater than the values reported by Bakker (1992). These discrepancies may be explained by the use of a different tank geometry including a flat-bottomed vessel and a different impeller-vessel configuration (diameter, off-the-bottom clearance ratio, ...).

The gassed to ungassed power ratio,  $P_g/P$ , against the gas flow number  $Fl$  for the Rushton turbine is plotted in Figure 2. The small and the medium spargers below the impeller induce a fall in the  $P_g/P$  ratio from 0.9 to 0.6. For the small sparger, this decrease is sudden and occurs at  $Fl = 0.025$ , whereas for the medium sparger the decrease in  $P_g/P$  is comparatively slow. The three large sparger configurations induce only a small decrease in the  $P_g/P$  ratio from 1 to 0.9 and thus have a higher gas handling capacity. This can be explained by the indirect loading of the impeller that occurs when a large sparger is used, whatever its position with respect to the impeller.

For the down-pumping A315 propeller (Figure 3), the use of spargers below the impeller firstly induces a plateau of the  $P_g/P$  ratio (at 1 for the small sparger and 0.9 for the medium and the large ones), and then a regular increase for  $Fl \geq 0.035$ . This can be explained by the direct opposition between the discharge flow of the propeller and the gas flow coming from the sparger. When the sparger is above the propeller, the  $P_g/P$  ratio decreases rapidly to 0.8 (small and medium sparger) or 0.9 (large sparger) and then remains at this value for all of the gas flow rates studied. There appears to be a small influence of the sparger diameter on  $P_g/P$ , however the position of the sparger with respect to the impeller is predominant.

The small and the large spargers located above the A315 propeller (Figure 4) in the up-pumping mode induce a regular increase of the  $P_g/P$  ratio from 1 to 1.2. As for the down-pumping impeller, this increase is due to the opposition between the discharge flow of the propeller and the gas flow coming from the sparger. However, when the sparger has the same diameter as the impeller, this phenomenon is not observed. Nevertheless, for this sparger and the spargers that are positioned below the impeller, the decrease in the  $P_g/P$  ratio upon gassing is minor. This indicates the good dispersion capacity of the impeller for the range of flow rates studied.

## Mass Transfer

Firstly, in order to verify the accuracy of the technique adopted for the measurement of  $k_L a$ , the results for the Rushton turbine with the small sparger placed below the impeller have been compared with the correlation reported by Van't Riet (1979):

$$k_L a = 0.026 \left( \frac{P_g}{V} \right)^{0.4} v_s^{0.5} \quad (6)$$

where  $P_g$  is the power consumption under aeration and  $v_s$  is the superficial gas velocity.

The average difference between the experimental and correlated results is approximately 4%, with the maximal difference being no greater than 8%. Considering this comparison, the experimental method employed in this work is considered to be valid for the range of operating conditions used.

### *Volumetric Mass Transfer Coefficients*

The evolution of the volumetric mass transfer coefficients as a function of the gas flow number for all of the sparger configurations studied with the Rushton turbine is shown in Figure 5. As expected, the mass transfer coefficients increase with an increasing gas flow number due to the increased gas holdup. Like for the  $P_g/P$  ratio, the more effective spargers are the large ones ( $D_S = 1.6D$ ) placed below or level with the impeller, the latter configuration discharging the gas in a downwards direction. For  $Fl \leq 0.05$ , the medium sparger ( $D_S = D$ ) enables  $k_La$  values similar to those given by the large spargers to be obtained. At larger gas flow numbers, however, this is no longer the case because the  $P_g/P$  ratio decreases, which indicates the beginning of the gas loading regime and therefore the gas handling capacity of the impeller decreases.

Figure 6 plots the volumetric mass transfer coefficient against the gas flow number for the A315 propeller in the down-pumping mode. Here, the highest  $k_La$  values are obtained with the spargers that also give the best gas handling capacities (the lowest fall in the  $P_g/P$  ratio), i.e. those which are placed below the impeller. The diameter of the sparger, however, has a much weaker influence on the  $k_La$ .

The results for the A315 propeller in the up-pumping mode are shown in Figure 7. Surprisingly, the best values of the volumetric mass transfer coefficient are obtained for the spargers which are situated below the impeller. It is only at high gas flow rates ( $Fl \geq 0.05$ ) that the medium sparger ( $D_S = D$ ) placed above the impeller enables  $k_La$  values, which are similar to those given with the spargers below the impeller, to be obtained. This can be explained by the smaller amount of gas that accumulates below the propeller when the gas is injected above the agitator (Figure 8(B)) compared with when the gas is injected below the impeller (Figure 8(A)). The differences in the gas distribution can be explained by the liquid flow fields generated by the up-pumping impeller. Two circulation loops are created, a strong one in the lower part of the tank and a weaker one in the upper part (Aubin, 2001). When the gas is injected below the impeller, the majority of it is entrained by the lower circulation loop and remains there for a considerable time. This was also observed by Aubin *et al.* (2004) for an up-pumping pitched blade turbine. When the sparger is placed above the impeller, however, the gas is entrained by both of the circulation loops. The gas that circulates in the upper loop escapes more rapidly to the



liquid surface, which decreases the bubble residence time and therefore the  $k_L a$ . In addition, the bubbles appear to be bigger when the spargers are placed above the impellers.

### *Overall Transfer Efficiency (OTE)*

The evolution of the overall transfer efficiency,  $OTE$ , as a function of the gas flow number,  $Fl$ , for each impeller and sparger configuration is shown in Figure 9, Figure 10 and Figure 11. For all of the configurations, the  $OTE$  increases with an increasing gas flow number. This is because as the gas flow rate increases, the  $k_L a$  also increases but the gassed power consumption decreases or remains more or less constant.

For the Rushton turbine, only the best configurations in terms of gas handling capacities (i.e. high  $P_g/P$  ratios) have been shown in Figure 9. The configuration with the large sparger below the turbine gives slightly higher  $OTE$  values than the other two configurations.

For the A315 propeller in the down-pumping mode, the  $OTE$  values for the small, medium and large spargers situated below the impeller are plotted in Figure 10. These spargers were shown to give the best results in terms of gas handling capacities and  $k_L a$ . For high gas flow rates,  $Fl > 0.04$ , the system with the medium sparger below the impeller is more efficient than the other configurations. For  $Fl < 0.04$ , however, the small and the medium spargers below the agitator give similar results.

The  $OTE$  values for the A315 propeller in the up-pumping mode, Figure 11, show a clear difference between the sparger configurations below and above the impeller: those located below the agitator give relatively higher efficiencies. Furthermore, the small sparger below the impeller gives consistently higher  $OTE$  values than the medium and large spargers. The difference in  $OTE$  values between the sparger positions corresponds directly to the fact that the configurations below the impeller give much higher  $k_L a$  values and that the  $P_g/P$  ratio for all configurations varies very little.

### *Comparison of the different impeller configurations*

For the sparger position below the impeller and for the three sparger diameters (small, medium and large), the performances of each impeller are compared together in terms of  $k_L a$  and  $OTE$ . For each characteristic quantity, the performance of the impellers studied can be summarized in decreasing superiority as the following.

*In terms of  $k_L a$ :*

Rushton turbine > A315 up-pumping mode > A315 down-pumping mode

*In terms of  $OTE$ :*

A315 up-pumping mode > A315 down-pumping mode > Rushton turbine

Overall, the  $k_{La}$  values for the Rushton turbine are much higher than those for the A315 propeller. Regardless of the sparger position, the  $k_{La}$  values for the radial turbine are in average 33% greater (small sparger) and 50% greater (medium and large spargers) than those obtained with the down-pumping A315. Comparison with the up-pumping A315 shows that the Rushton turbine gives  $k_{La}$  values which are 30% greater than the former impeller for all sparger diameters. This is explained by the fact that the experiments were carried out at a constant rotational speed and not at constant power dissipation. Since the  $k_{La}$  is a function of gassed power consumption, the Rushton turbine has a much larger mass transfer coefficient because it dissipates significantly more power than the other impellers studied at constant impeller speed. For the A315 propeller, the up-pumping configuration gives  $k_{La}$  values which are approximately 20% greater than those obtained in the down-pumping mode.

It can be seen that when using the *OTE* as a comparison criterion, the Rushton turbine has the lowest performance in terms of mass transfer efficiency, compared with the other impellers. Even though the Rushton turbine enables a large quantity of oxygen to be transferred quickly to the liquid phase, it requires a large amount of power for carrying out the process. In comparison, the *OTE* values of the A315 propeller in up- or down-pumping mode are approximately 1- 1.5 times greater than those of the Rushton turbine. Looking at the effect of axial pumping direction for the A315 propeller on the *OTE* shows that the up-pumping mode gives higher values than the down-pumping mode: 10% greater for the medium sparger, 20% for the large and 35% for the small one. More details on the comparison between different radial and axial agitators can be found in Sardeing *et al.* (2003).

## CONCLUSIONS

This paper deals with the gas-liquid mass transfer performance of various sparger configurations in combination with a down- and an up-pumping axial flow impeller (A315 propeller) and a radial flow impeller (Rushton turbine). For each impeller, the sparger configurations that give the best performance in terms of gas handling capacity,  $k_{La}$  and *OTE* are summarised in Table 4.

By merging the information of the three columns in Table 4, the adequate sparger for each impeller can be proposed:

*Rushton turbine:*

Large sparger ( $D_S > D$ ) below the impeller or

Large sparger discharging gas downwards ( $D_S > D$ ) level with the impeller

*A315 propeller in down-pumping mode:*

Medium sparger ( $D_S = D$ ) located below the impeller

This configuration is preferred over the small and large spargers located below the agitator because it gives equivalent or better performances in terms of  $k_L a$  and  $OTE$ . Furthermore, the  $P_g/P$  ratio for this configuration remains between 0.8 and 1, which means that it is not flooded at high gas rates.

*A315 propeller in up-pumping mode:*

Small ( $D_S < D$ ), medium ( $D_S = D$ ) and large ( $D_S > D$ ) spargers located below the impeller

The spargers positioned below the impeller are preferred for their  $k_L a$  and  $OTE$  performances, whilst losing little power upon gassing.

In general, it can be concluded that the sparger diameter does not have a very important effect on the mass transfer performance of the impellers studied, although it appears that for the most part a sparger diameter equal to or larger than the impeller diameter is preferable, whatever the type of agitator. The sparger position, on the other hand, has an important effect on mass transfer. The results of this study indicate that it is most advantageous to position the sparger in a location which favours the gas to be entrained into the circulation loop present in the lower part of the tank. The gas then has a longer residence time in the vessel, which promotes mass transfer.

The comparison of impeller types shows that the Rushton turbine gives the highest  $k_L a$  values but is the least efficient impeller in terms of  $OTE$  values due to its relatively high power consumption. The most energy efficient impeller for mass transfer, on the other hand, is the A315 propeller in the up-pumping mode. Although, the mass transfer performance of the down-pumping A315 propeller is less than in the up-pumping mode.

Future work will concentrate on the local measurement of gas hold-up and bubble diameters in order to better understand the phenomena observed in this work. The influence of the distance between the axial impeller and the sparger positioned above it has also to be investigated.

## **NOMENCLATURE**

*A315D* A315 propeller in down-pumping mode

*A315U* A315 propeller in up-pumping mode

$C$  impeller clearance (m)

$C_s$  sparger clearance (m)

$C_t$	dissolved oxygen concentration at time $t$ ( $\text{kg.m}^{-3}$ )
$C_0$	dissolved oxygen concentration at $t = 0$ ( $\text{kg.m}^{-3}$ )
$C^*$	oxygen concentration at saturation ( $\text{kg.m}^{-3}$ )
$D$	impeller diameter (m)
$D_s$	sparger diameter (m)
$D_T$	tank diameter (m)
$H$	liquid height in tank (m)
$k_L a$	volumetric mass transfer coefficient ( $\text{s}^{-1}$ )
$N$	impeller rotational speed ( $\text{s}^{-1}$ )
$P$	ungassed impeller power consumption (W)
$P_g$	gassed impeller power consumption (W)
$P_o$	Dimensionless power number (-)
$Q_G$	gas flow rate ( $\text{m}^3 \text{ s}^{-1}$ or vvm)
$Q_{O_2}$	mass flow rate of oxygen ( $\text{kg. s}^{-1}$ )
$s$	shaft diameter (m)
$t$	time (s)
$T$	temperature ( $^{\circ}\text{C}$ )
$\tau$	response time of the oxygen probe (s)
$v_s$	superficial gas velocity ( $\text{ms}^{-1}$ )
$V$	volume of liquid in the tank ( $\text{m}^3$ )
$\rho$	liquid density ( $\text{kg.m}^{-3}$ )

## REFERENCES

- Aubin, J., 2001, Mixing Capabilities of Down- and Up-Pumping Axial Flow Impellers in Single Phase and Gas-Liquid Systems: Experimental and CFD Studies, PhD Thesis, INPT France & The University of Sydney Australia.
- Aubin, J., Le Sauze, N., Bertrand, J., Fletcher, D.F. and Xuereb, C., 2004, 'PIV Measurements of Flow in an Aerated Tank Stirred by a Down- and an Up-Pumping Axial Flow Impeller', *Experimental Thermal & Fluid Sci.*, 28, 447-456.

- Bakker, A., 1992, *Hydrodynamics of Gas-Liquid Dispersions*, PhD Thesis, Delft University of Technology, Delft, Holland.
- Bakker, A. and Van den Akker, H.E.A., 1994, 'Gas-Liquid Contacting with Axial Flow Impellers', *Trans IChemE, Part A, Chem Eng Res Des*, 72(A): 573-582.
- Bertrand, J., Couderc, J.P. and Angelino, H., 1980, 'Power Consumption, Pumping Capacity and Turbulence Intensity in Baffled Stirred Tanks: Comparison Between Several Turbines', *Chem Eng Sci*, 35(10): 2157-2163.
- Birch, D. and Ahmed, N., 1996, 'Gas Sparging in Vessels Agitated by Mixed Flow Impellers', *Powder Tech*, 88: 33-38.
- Birch, D. and Ahmed, N., 1997, 'The Influence of Sparger Design and Location on Gas Dispersion in Stirred Vessels', *Trans IChemE, Part A, Chem Eng Res Des*, 75(A): 487-496.
- Bouaifi, M. and Roustan, M., 1998, 'Bubble Size and Mass Transfer Coefficients in Dual-Impeller Agitated Reactors', *Can J Chem Eng*, 76: 390-397.
- Breucker, Ch., Steiff A. and Weinspach, P.-M., 1988, 'Interaction Between Stirrer, Sparger and Baffles Concerning Different Mixing Problems', *Proc. 6<sup>th</sup> European Conf. on Mixing*, Pavia, Italy, BHRA Fluid
- Lopes de Figueiredo, M.M. and Calderbank, P.H., 1979, 'The Scale-Up of Aerated Mixing Vessels for Specified Oxygen Dissolution Rates', *Chem Eng Sci*, 34: 1333-1338.
- McFarlane, C.M., Zhao, X.-M. and Nienow, A.W., 1995, 'Studies of High Solidity Ratio Hydrofoil Impellers for Aerated Bioreactors. 2. Air-Water Studies', *Biotechnol. Prog.*, 11: 608-618.
- Nienow, A.W., Haozhong, W., Huoxing, L. and Allsford, K.V., 1986, 'The Advantage of Using Large Ring Spargers with Standard Rushton Turbines in Gassed Reactors', Paper 8k-202, *World Congress III of Chemical Engineering*, Tokyo, 3: 354-357.
- Rewatkar, V.B., Deshpande, A.J., Pandit, A.B. and Joshi, J.B., 1993, 'Gas Hold-up Behavior of Mechanically Agitated Gas-Liquid Reactors Using Pitched Blade Downflow Turbines.', *Can J Chem Eng*, 71: 226-237.
- Rewatkar, V.B., Raghava Rao, K.S.M.S. and Joshi, J.B., 1991, 'Critical Impeller Speed for Solid Suspension in Mechanically Agitated Three-Phase Reactors. 1. Experimental Part.', *Ind Eng Chem Res*, 30: 1770-1784.
- Rewatkar, V.B. and Joshi, J.B., 1991a, 'Role of Sparger Design in Mechanically Agitated Gas-Liquid Reactors. Part I: Power Consumption.', *Chem Eng Technol*, 14: 333-347.
- Rewatkar, V.B. and Joshi, J.B., 1991b, 'Role of Sparger Design in Mechanically Agitated Gas-Liquid Reactors. Part II: Liquid Phase Mixing.', *Chem Eng Technol*, 14: 386-393.

- Rewatkar, V.B. and Joshi, J.B., 1993, 'Role of Sparger Design on Gas Dispersion in Mechanically Agitated Gas-Liquid Contactors.', *Can J Chem Eng*, 71: 278-291.
- Sardeing, R., Aubin, J. and Xuereb, C., 2003, 'Gas-Liquid Mass Transfer: A Comparison of Down- and Up-Pumping Axial Flow Impellers with Radial Impellers.', submitted to *Chem Eng Res Des*, (A).
- Van't Riet, K., 1979, 'Review of Measuring Methods and Results in Non-Viscous Gas-Liquid Mass Transfer in Stirred Vessels', *Ind Eng Chem Process Des Dev*, 18(3): 357-364.

## LIST OF TABLES

Table 1: Characteristics and name of sparger configurations.

Table 2: Sparger configurations studied for each impeller.

Table 3: Comparison of ungassed power numbers for the different impellers studied. <sup>a</sup>Bertrand *et al.* (1980); <sup>b</sup>Bakker (1992); <sup>c</sup>Aubin (2001).

Table 4: Spargers giving the best results in terms of gas handling and mass transfer capacities.

<b>Sparger position</b>	Above the impeller	Level the impeller	Below the impeller
$C_s$	0.2C	C	1.6C
<b>Gas discharge direction</b>	Towards the impeller	2 cases, see below	Towards the impeller
<b>Sparger size</b>			
Small size $D_s = 0.6D$	S-a		S-b
Medium size $D_s = D$	M-a		M-b
Large size $D_s = 1.6D$	L-a	<i>Gas discharged upwards: L-l-up</i> <i>Gas discharged downwards: L-l-down</i>	L-b

Table 1



<b>Agitator</b>	<b>Configurations studied</b>
Rushton turbine	S-b / M-b / L-b / L-l-down / L-l-up
A315 propeller down-pumping mode	S-b / M-b / L-b / S-a / M-a / L-a
A315 propeller up-pumping mode	S-b / M-b / L-b / S-a / M-a / L-a

Table 2

<b>Impeller type</b>	<b><math>P_0</math> – This work (Error <math>\pm 5</math> %)</b>	<b><math>P_0</math> – Literature</b>
Rushton turbine	4.6	4.9 <sup>a</sup>
A315D	1.32	0.76 <sup>b</sup> – 1.26 $\pm$ 0.05 <sup>c</sup>
A315U	1.34	1.17 $\pm$ 0.07 <sup>c</sup>

Table 3

<b>Sparger giving the best results in terms of:</b>				
<b>Impeller</b>	<b><math>P_g/P</math> ratio</b>	<b><math>k_L a</math></b>	<b>OTE</b>	<b>Recommended sparger</b>
Rushton turbine	L-b $\approx$ L-l-down $\approx$ L-l-up	$Fl \leq 0.05$ M-b $\approx$ L-b $\approx$ L-l-down $Fl > 0.05$ L-b $\approx$ L-l-down	L-b $\approx$ L-l-down	L-b $\approx$ L-l-down
A315 down-pumping	S-b $\approx$ M-b $\approx$ L-b	S-b $\approx$ M-b $\approx$ L-b	$Fl < 0.04$ M-b $\approx$ L-b $Fl > 0.04$ M-b	M-b
A315 up-pumping	S-b $\approx$ M-b $\approx$ L-b $\approx$ S-a $\approx$ M-a $\approx$ L-a	S-b $\approx$ M-b $\approx$ L-b	S-b $\approx$ M-b $\approx$ L-b	S-a $\approx$ M-a $\approx$ L-a

Table 4

## LIST OF FIGURES

Figure 1: Schematic diagram of the experimental arrangement.

Figure 2: Evolution of the gassed to ungassed power ratio with increasing gas flow rate for the Rushton turbine with the different sparger configurations.

Figure 3: Evolution of the gassed to ungassed power ratio with increasing gas flow rate for the A315 propeller in down-pumping configuration with the different sparger configurations.

Figure 4: Evolution of the gassed to ungassed power ratio with increasing gas flow rate for the A315 propeller in up-pumping configuration with the different sparger configurations.

Figure 5: Volumetric mass transfer coefficients as a function of the gas flow number at constant impeller speed ( $N = 5 \text{ s}^{-1}$ ) for the Rushton turbine with the different sparger configurations.

Figure 6: Volumetric mass transfer coefficients as a function of the gas flow number at constant impeller speed ( $N = 5 \text{ s}^{-1}$ ) for the A315 propeller in the down-pumping mode with the different sparger configurations.

Figure 7: Volumetric mass transfer coefficients as a function of the gas flow number at constant impeller speed ( $N = 5 \text{ s}^{-1}$ ) for the A315 propeller in the up-pumping mode with the different sparger configurations.

Figure 8. Photographs of the gas dispersion obtained with the A315 propeller in the up-pumping mode with the small sparger below the impeller (A) and above the impeller (B) for  $Fl = 0.075$ .

Figure 9. Overall Transfer Efficiency (*OTE*) as a function of the gas flow number at constant impeller speed ( $N = 5 \text{ s}^{-1}$ ) for the Rushton turbine with the different sparger configurations.

Figure 10. Overall Transfer Efficiency (*OTE*) as a function of the gas flow number at constant impeller speed ( $N = 5 \text{ s}^{-1}$ ) for the A315 propeller in the down-pumping mode with the different sparger configurations.

Figure 11. Overall Transfer Efficiency (*OTE*) as a function of the gas flow number at constant impeller speed ( $N = 5 \text{ s}^{-1}$ ) for the A315 propeller in the up-pumping mode with the different sparger configurations.

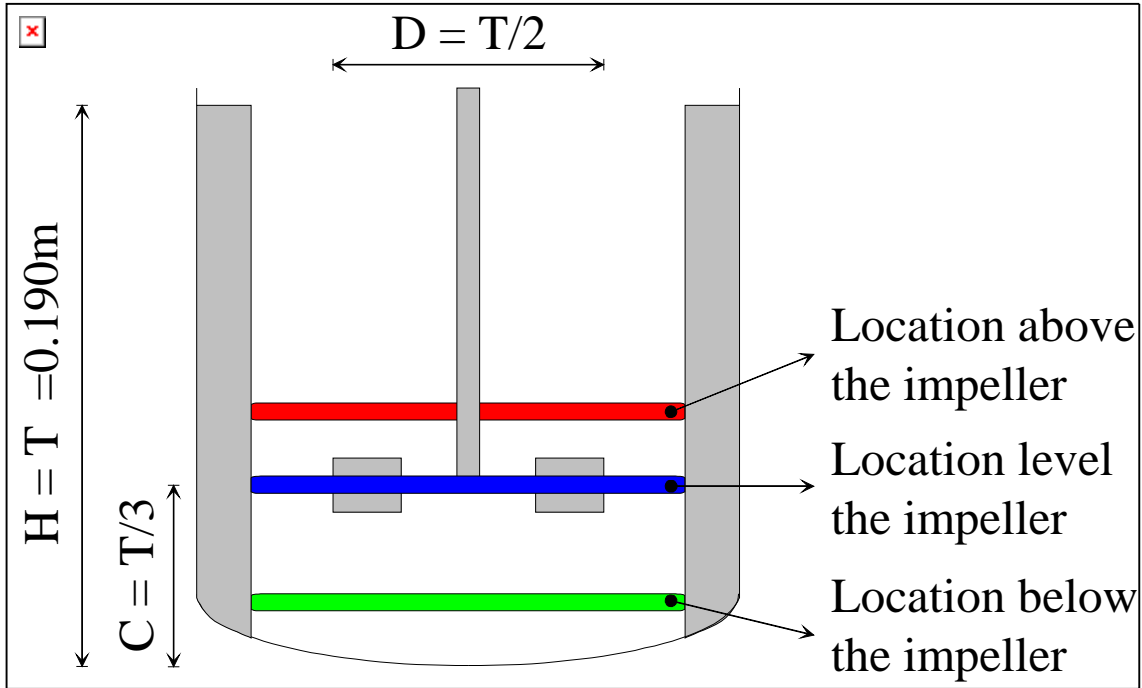


Figure 1

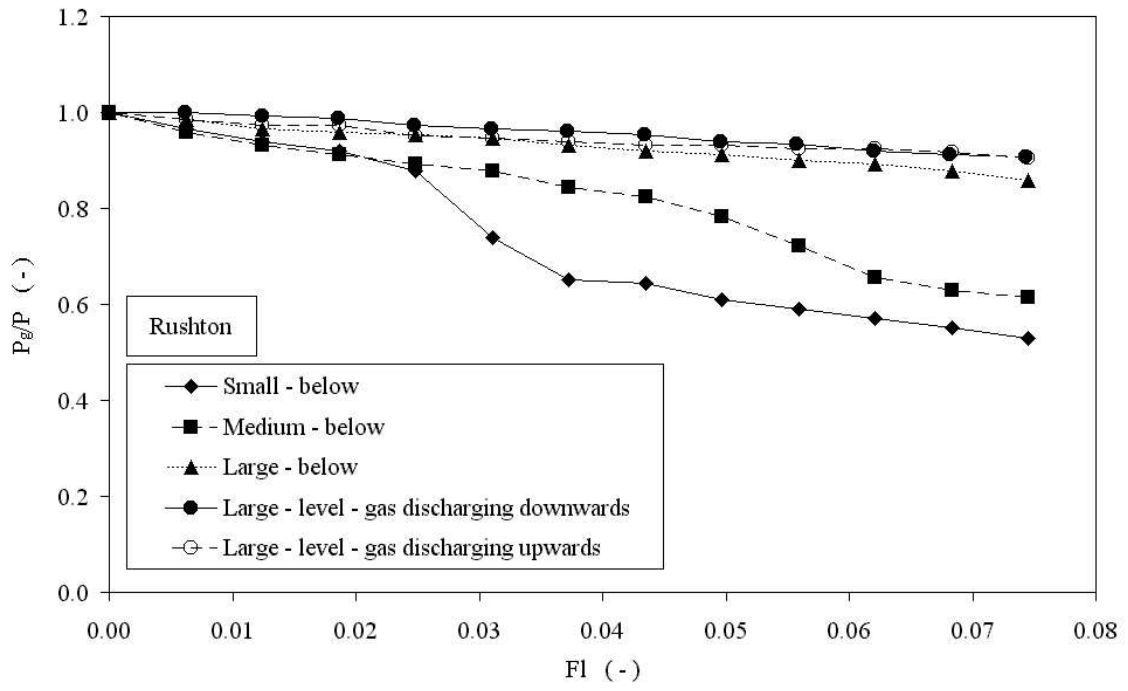


Figure 2

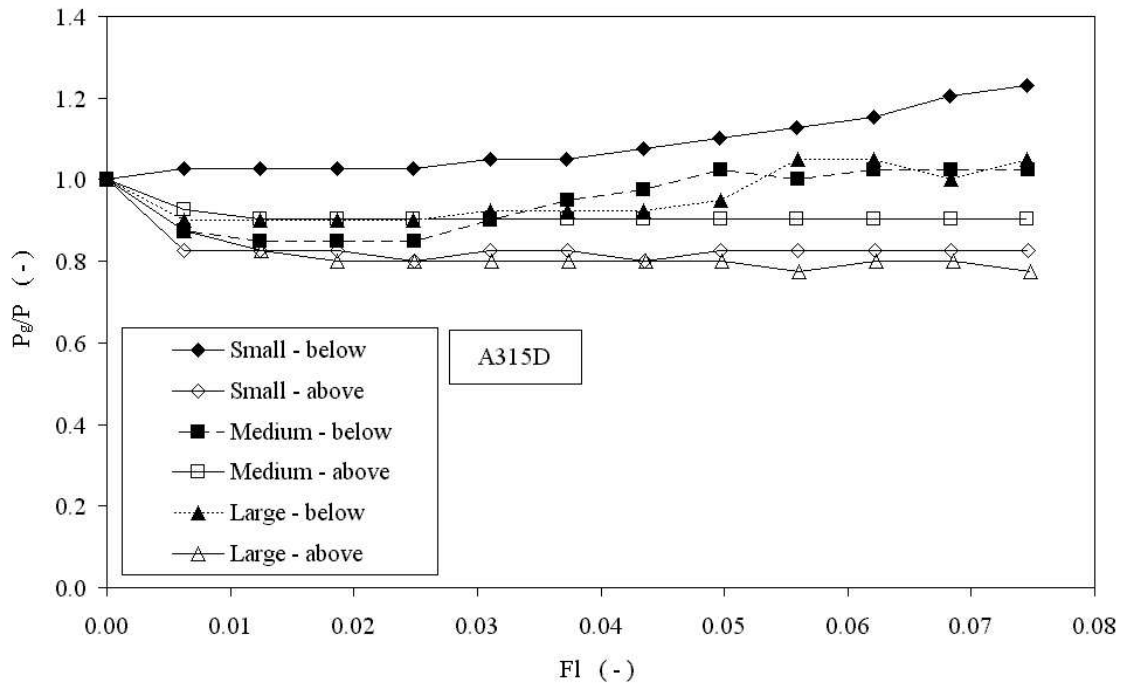


Figure 3

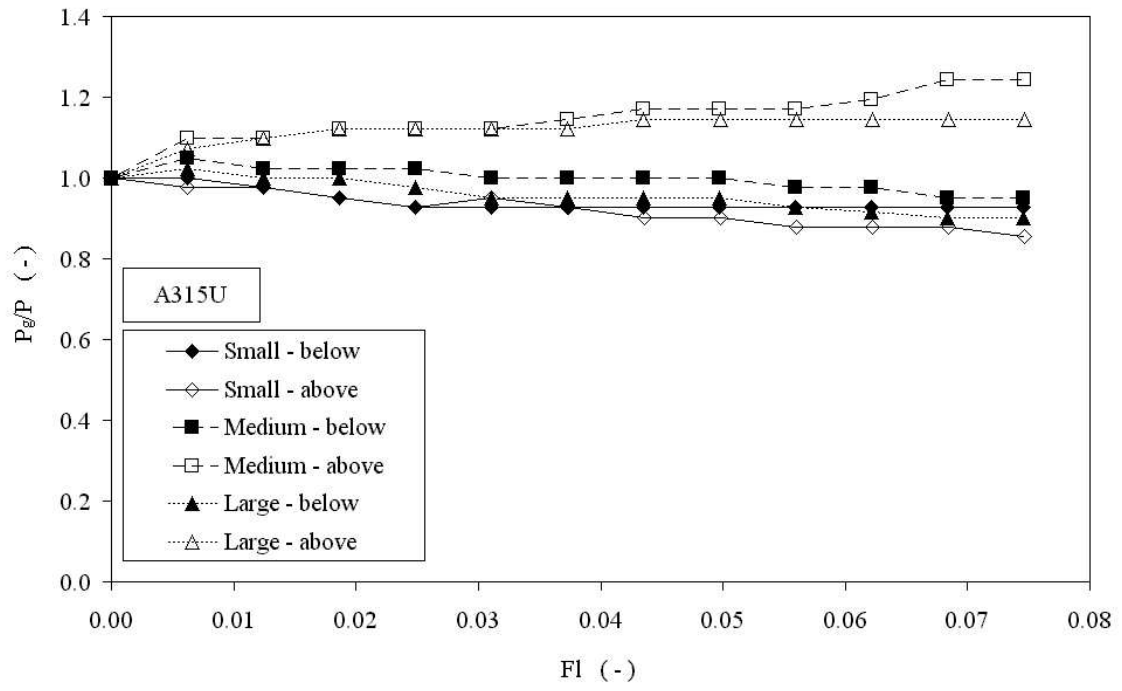


Figure 4



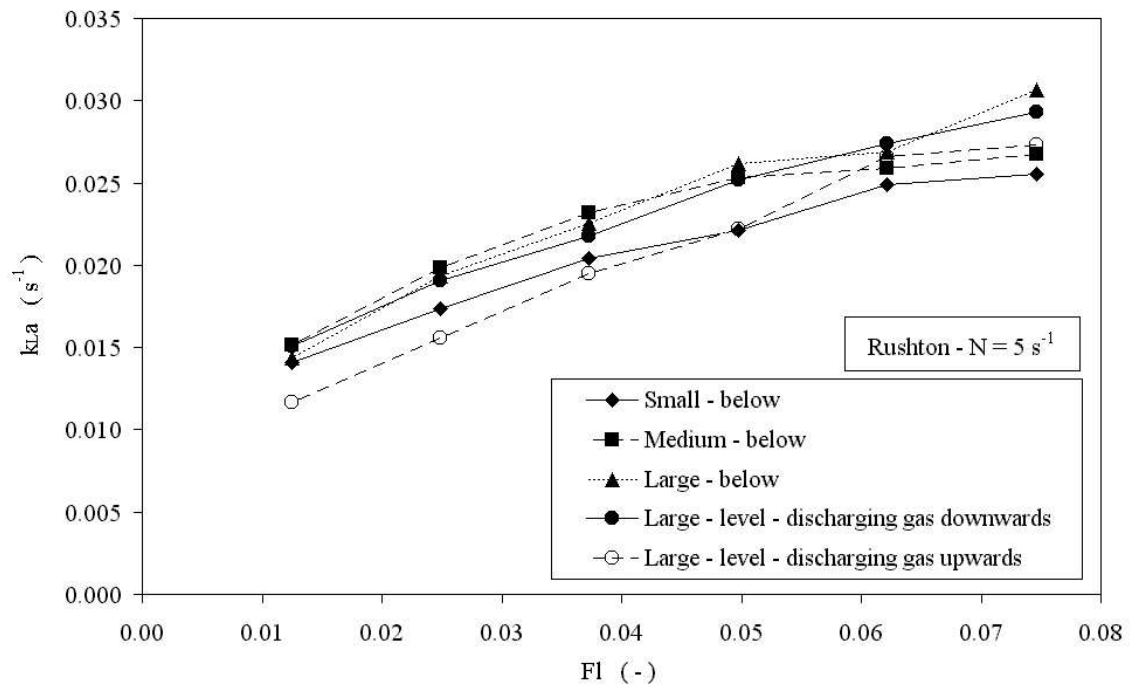


Figure 5

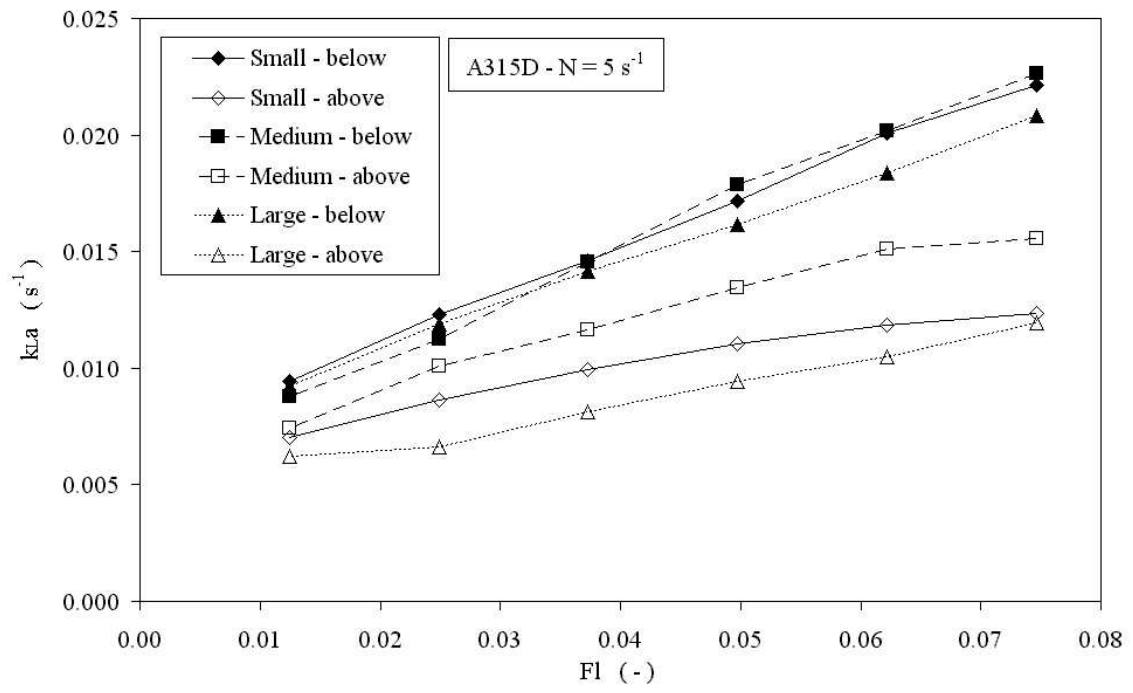


Figure 6

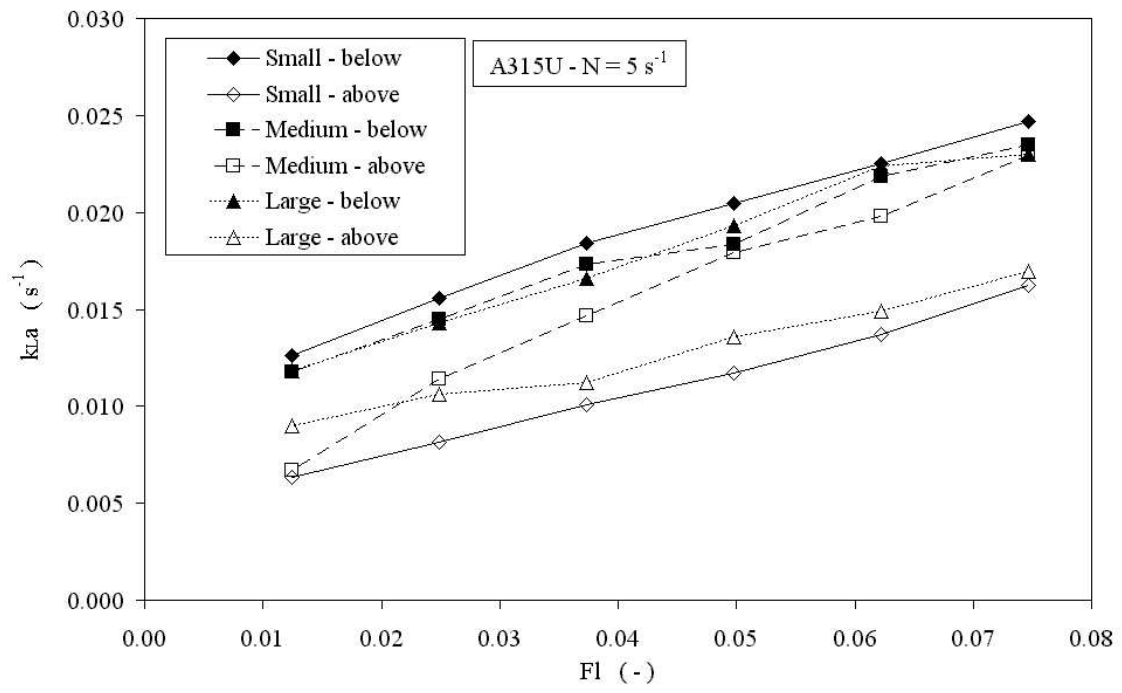
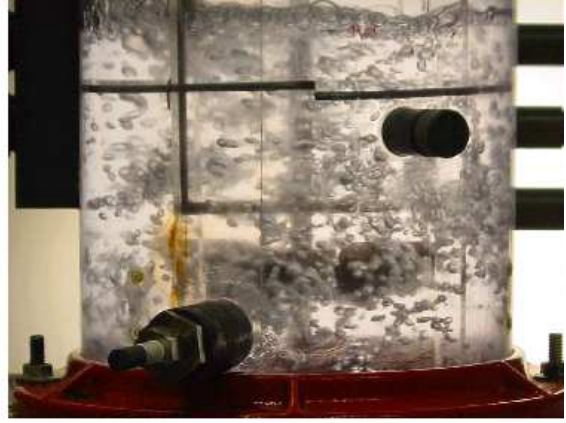


Figure 7



A



B

Figure 8

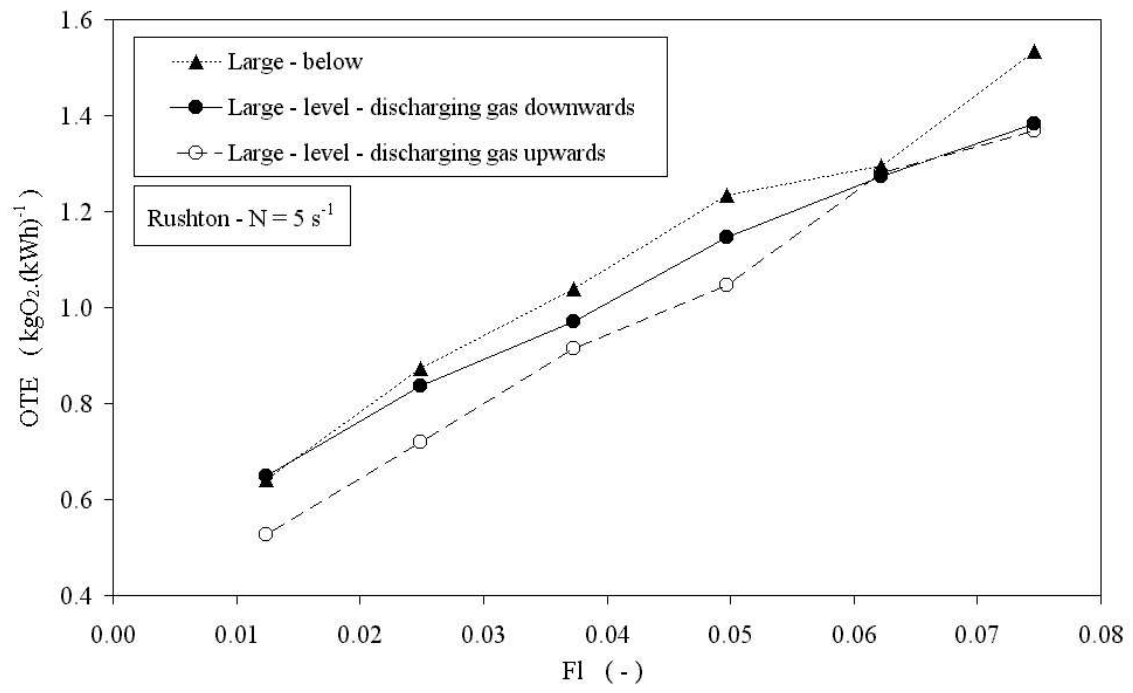


Figure 9

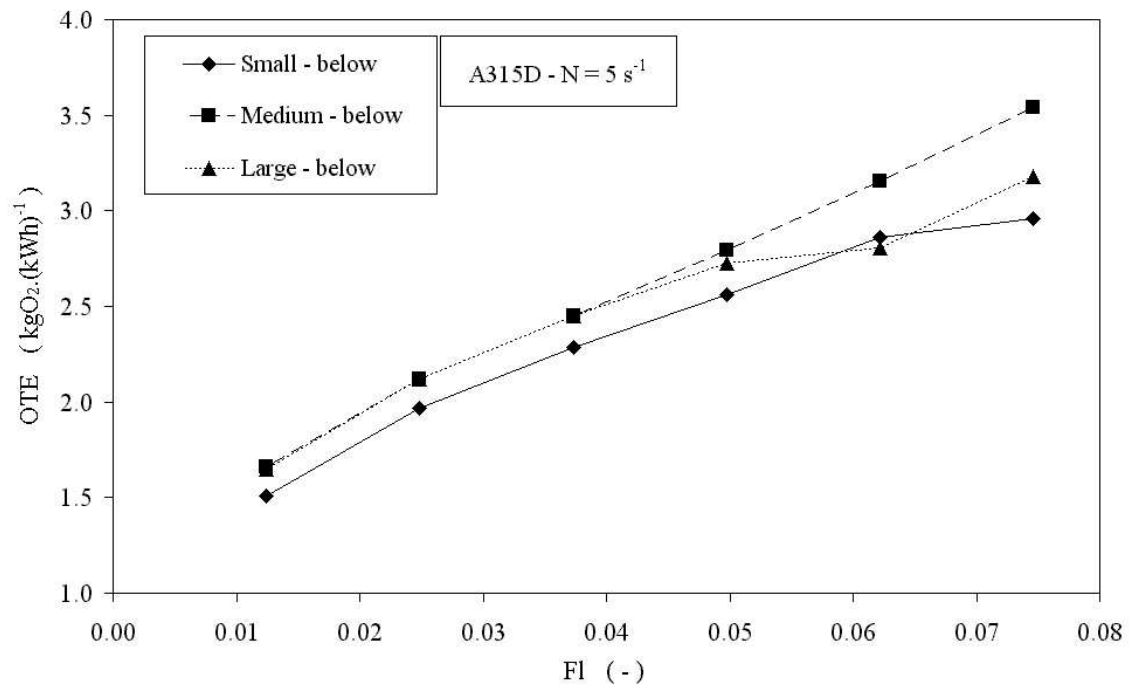


Figure 10

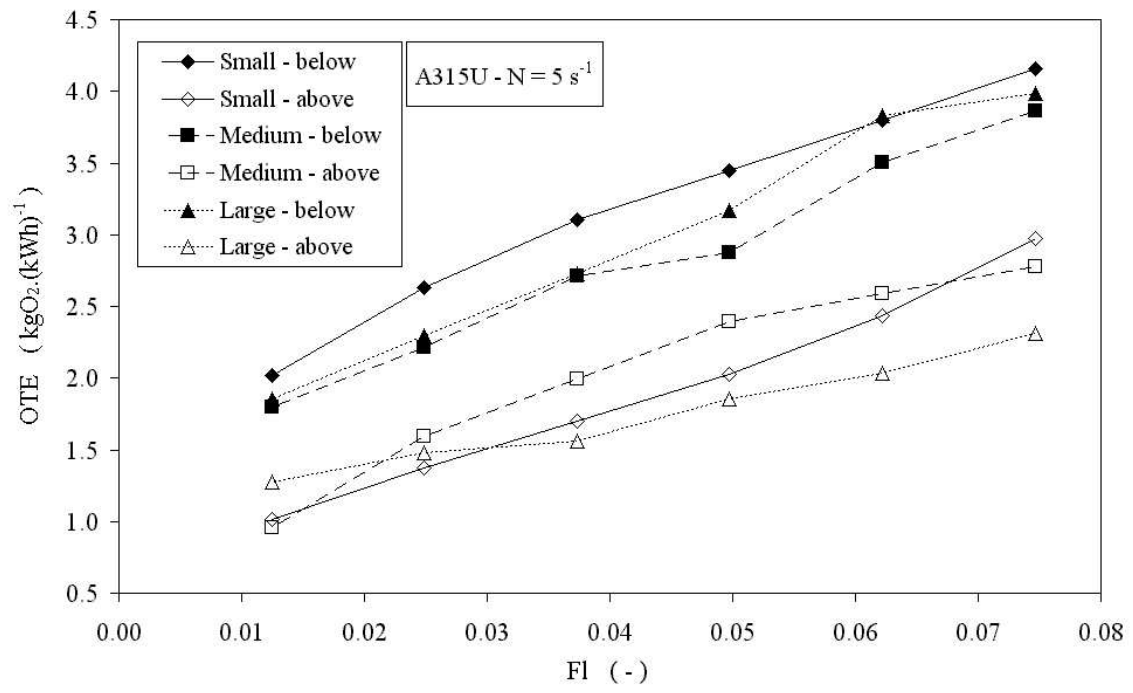


Figure 11